Hyaluronan deposition in islets may precede and direct the location of islet immune-cell infiltrates

Marika Bogdani[1], **Cate Speake**[2], **Mathew J. Dufort**[3], **Pamela Y. Johnson**[1], **Megan J. Larmore**[4], **Anthony J. Day**[5], **Thomas N. Wight**[1], **Åke Lernmark**[6,7], **Carla J. Greenbaum**[2]

[1]Matrix Biology Program, Benaroya Research Institute, Virginia Mason, 1201 9th Avenue, Seattle, WA 98101, USA

[2]Diabetes Research Program and Clinical Research Center, Benaroya Research Institute at Virginia Mason, Seattle, WA, USA

[3]Bioinformatics department, Benaroya Research Institute, Virginia Mason, Seattle, WA, USA

[4]Histology and Imaging Core, University of Washington, Seattle, WA, USA

[5]Wellcome Trust Centre for Cell-Matrix Research, University of Manchester, Manchester, UK

[6]Department of Medicine, University of Washington, Seattle, WA, USA

[7]Present address: Department of Clinical Sciences, Lund University/CRC, Skåne University Hospital, Malmö, Sweden

Abstract

Aims/hypothesis—Substantial deposition of the extracellular matrix component hyaluronan (HA) is characteristic of insulitis in overt type 1 diabetes. We investigated whether HA accumulation is detectable in islets early in disease pathogenesis and how this affects the development of insulitis and beta cell mass.

Methods—Pancreas tissue from 15 non-diabetic organ donors who were positive for islet autoantibodies (aAbs) and from 14 similarly aged aAb⁻ control donors were examined for the amount of islet HA staining and the presence of insulitis. The kinetics of HA deposition in islets, along with the onset and progression of insulitis and changes in beta cell mass, were investigated in BioBreeding DR*Lyp/Lyp* rats (a model of spontaneous autoimmune diabetes) from 40 days of age until diabetes onset.

Results—Abundant islet HA deposits were observed in pancreas tissues from n=3 single- and n=4 double-aAb$^+$ donors (aAb$^+$HA^{high}). In these seven tissues, the HA-stained areas in islets measured 1000±240 μm^2 (mean±SEM) and were fourfold larger than those from aAb$^-$ control samples. The aAb$^+$HA^{high} tissues also had a greater prevalence of islets that were highly rich in HA (21% of the islets in these tissues contained the largest HA-stained areas [>2000 μm^2] vs less than 1% in tissues from aAb$^-$ control donors). The amount of HA staining in islets was associated with the number of aAbs (i.e. single- or double-aAb positivity) but not with HLA genotype or changes in beta cell mass. Among the seven aAb$^+$HA^{high} tissues, three from single- and one from double-aAb$^+$ donors did not show any islet immune-cell infiltrates, indicating that HA accumulates in aAb$^+$ donors independently of insulitis. The three aAb$^+$HA^{high} tissues that exhibited insulitis had the largest HA-stained areas and, in these tissues, islet-infiltrating immune cells co-localised with the most prominent HA deposits (i.e. with HA-stained areas >2000 μm^2). Accumulation of HA in islets was evident prior to insulitis in 7–8-week-old presymptomatic DR*Lyp/Lyp* rats, in which the islet HA-stained area measured 2370±170 μm^2 (mean±SEM), which was threefold larger than in 6-week-old rats. This initial islet HA deposition was not concurrent with beta cell loss. Insulitis was first detected in 9–10-week-old rats, in which the HA-stained areas were 4980±500 μm^2. At this age, the rats also exhibited a 44% reduction in beta cell mass. Further enlargement of the HA-positive areas (mean±SEM: 7220±880 μm^2) was associated with invasive insulitis. HA deposits remained abundant in the islets of rats with destructive insulitis, which had lost 85% of their beta cells.

Conclusions/interpretation—This study indicates that HA deposition in islets occurs early in type 1 diabetes and prior to insulitis, and points to a potential role of HA in triggering islet immune-cell infiltration and the promotion of insulitis.

Introduction

The process of beta cell damage in type 1 diabetes starts long before the disease becomes overt, and is influenced by both genetic and environmental factors [1, 2]. The early stage of disease pathogenesis is characterised by islet autoimmunity, marked by two or more of the four currently identified type 1 diabetes-associated islet autoantibodies (aAbs; against insulin, GAD65, islet tyrosine phosphatase 2 [IA-2] or zinc transporter 8 [ZnT8]), followed by increasing beta cell dysfunction and death, and then clinically apparent disease [1, 3–8]. A histopathological hallmark of diabetes at the time of clinical onset is insulitis, an inflammatory cell infiltrate indicating an ongoing immune-cell mediated process in islets that, presumptively, results in beta cell destruction [9–15]. At present, what guides immune-cell trafficking from the blood into islets is not known. Moreover, the initial changes in human islets that trigger the recruitment of immune cells have not been defined.

We have proposed that an increase in the amount of hyaluronan (HA), a major component of the islet extracellular matrix (ECM), takes place early in the natural course of type 1 diabetes, and that HA accumulation promotes islet invasion by immune cells and functional impairment of beta cells [16, 17]. HA, a linear high-molecular-weight polysaccharide,

amasses at sites of inflammation and has become recognised as a regulator of several aspects of inflammation, including leucocyte migration, angiogenesis and the generation of inflammatory cytokines [18–20]. Our previous observations of abundant HA in insulin-deficient islets and regions of insulitis in type 1 diabetes establish a link between HA accumulation in islets, beta cell loss and insulitis [16]. However, this association is based on changes in islet resulting from a chronic process that has been ongoing for months to years. Whether islet HA accumulation is an early event in type 1 diabetes pathogenesis and how it influences the development of insulitis is not known. To address this question, we investigated the occurrence and distribution of islet HA deposits in the presence or absence of insulitis in pancreas tissues from non-diabetic aAb$^+$ organ donors. In addition, we evaluated the kinetics of HA accumulation in islets concurrently with the extent of islet immune-cell infiltration and changes in beta cell mass in presymptomatic BioBreeding (BB) DR*Lyp/Lyp* rats during the progression to hyperglycaemia.

Methods

Donors and tissue procurement

Pancreas tissues samples from non-diabetic organ donors were obtained through the Network for Pancreatic Organ Donors with Diabetes (nPOD). Samples were from n=10 single-aAb$^+$ and n=5 double-aAb$^+$ donors, and n=14 similarly aged control aAb$^-$ donors. Clinical characteristics of the donors are shown in electronic supplementary material (ESM) Table 1 (note that this study did not involve isolated human islets, but paraffin sections prepared from formalin-fixed paraffin-embedded pancreas tissues from organ donors). For each donor, we randomly sampled six paraffin blocks from different regions of the pancreas. The pancreas tissues are referred to, henceforth, as 'tissues'. All the experiments were carried out with the approval of the Institutional Review Board of the Benaroya Research Institute. The investigators were not blind to the group assignment since the tissues were obtained as they became available, and the donor aAb status was known by the investigators. However, the investigators were blind to aAb status during data collection.

BB DR rats

The BB rat model of autoimmune diabetes shares characteristics common to human disease, including spontaneous hyperglycaemia, ketoacidosis, genetic susceptibility and insulitis [21]. Male and female BB DR+/+, DR*Lyp*/+, and DR*Lyp/Lyp* rats [22] were obtained from Å. Lernmark at the University of Washington (Seattle, WA, USA). The rats were housed in a specific-pathogen-free facility at the University of Washington on a 12-h light/dark cycle and were fed a regular diet (Harlan Teklad, Madison, WI, USA) and given water ad libitum. Diabetes develops spontaneously by 12 weeks of age in DR*Lyp/Lyp* rats, while the diabetes-resistant (DR+/+ and DR*Lyp*/+) rats remain diabetes-free throughout life [22, 23]. The colony was maintained by intercrossing DR*Lyp*/+ rats. These crosses generated DR*Lyp/Lyp* rats as well as DR*Lyp*/+ and DR+/+ controls. The DR*Lyp*/+ and DR+/+ control rats had similar body weight, glucose levels and islet morphology at all ages. The body weight and blood glucose for each individual rat was recorded daily, from 40 days of age until DR*Lyp/Lyp* rats became diabetic (blood glucose levels 14 mmol/l). Rat pancreases were processed for histological analysis or hormone assay. All animal studies were approved by

the Institutional Animal Care and Use Committee of the University of Washington and the Benaroya Research Institute.

Histochemistry and immunohistochemistry

Staining methodologies were performed as previously described [17]. Serial sections were prepared from all the paraffin blocks. Sections were stained for HA using a biotinylated HA binding protein prepared from cartilage [24]. The primary antibodies used for immunohistochemistry are listed in ESM Table 2. The primary and secondary antibodies were diluted in PBS (ThermoFisher, Waltham, MA, USA). Positive and negative controls were included in each staining experiment. Sections were examined using a Leica DM IRB microscope (Wetzlar, Germany), and images were acquired using a Spot Xplorer camera and imaging software (Sterling Heights, MI, USA).

Morphometric analysis and quantification

Whole-section bright-field imaging was performed as previously described [17, 23]. Islets were identified by their staining for synaptophysin (SYN). Thirty per cent of the human islets were sampled according to assumption-free systematic uniform random sampling (based on our pilot studies, which indicate that this sampling results in a coefficient of error <2%). We classified HA$^+$ areas in islets using an established categorisation scheme with the following categories: 100, 101–500, 501–1000, 1001–2000, and >2000 μm^2 per islet [17, 25, 26]. Tissues from aAb$^+$ donors, with a mean - islet HA-stained area significantly larger than that of the aAb$^-$ controls, were defined as aAb$^+$HA^{high} or as having HA deposits, while tissues with islet HA-stained areas that were similar in size to those of the controls were defined as aAb$^+$HA^{low}.

Evaluation of islet immune-cell infiltrates

Sections were stained for leucocyte common antigen (LCA) and SYN to detect islet-infiltrating immune cells. All islets present in the sections were examined. Islets were counted along with the number of LCA$^+$ cells in contact with endocrine cells [17, 22]. Human islet immune-cell infiltrates were evaluated by determining: (1) the percentage of islets with LCA$^+$ cells adjacent to endocrine cells; and (2) the number of LCA$^+$ cells per islet that were adjacent to endocrine cells. Tissues exhibiting 15 LCA$^+$ cells in contact with endocrine cells per islet [9, 27] were defined as LCA^{high}. In DR*Lyp/Lyp* rats, insulitis is a continuum from scarce to numerous immune cells. Immune cells first appear at the islet periphery and subsequently invade the whole islet. In these rats, insulitis was evaluated according to the presence and the extent of islet LCA$^+$ cell infiltration and was graded as follows: grade 0, no infiltration; grade 1, LCA$^+$ cells present around islets and within the islets in <25% of the islet area; grade 2, LCA$^+$ cells occupying 75% of the islet area; grade 3, LCA$^+$ cells infiltrating >75% of the islet or the islets are devoid of beta cells. Each islet in an individual rat was examined once and assigned an insulitis grade; the grade of highest prevalence determined the insulitis grade for that rat (ESM Table 3). Control DR*Lyp*/+ and DR+/+ rats do not develop insulitis.

Quantification of islet mass, beta cell mass, proliferation and apoptosis

One section for each of the paraffin blocks sampled per human pancreas was stained for Ki67/insulin to determine beta cell proliferation rate and to measure the relative insulin$^+$ area. Four sections per pancreas were stained for TUNEL/insulin to determine apoptosis rate. The TUNEL stain (Millipore, Burlington, MA, USA) was performed according to the manufacturer's instructions. For each rat, consecutive pancreas sections were stained for SYN (eight sections per rat, 400 μm apart) and insulin (eight sections per rat, 400 μm apart) to measure the relative pancreas islet and beta cell areas at 100% sampling using Visiopharm software (Hoersholm, Denmark). The relative positive areas were then multiplied by the pancreas weight to determine islet or beta cell mass.

Statistical analysis

Data are expressed as mean ± SEM of *n* independent measurements. The significance of the difference between two or more groups of data was evaluated using the Mann–Whitney *U* test, Kruskal–Wallis test or ANOVA. Correlation analysis was performed using the nonparametric Spearman's rank correlation test. A *p* value of less than 0.05 was considered statistically significant. All analyses were performed using GraphPad Prism version 7.00 for Windows (GraphPad Software, San Diego, CA, USA).

Results

Abundant islet HA deposits form in a subset of aAb$^+$ donors

While HA was detectable extracellularly in islets from all tissues, islets from aAb$^+$ donors exhibited HA deposits, defined by the greater areas of HA staining vs controls (Fig. 1). Examination of 4598 islets from 14 aAb$^-$ and 5482 islets from 15 aAb$^+$ donors indicated a 2.8-fold larger islet HA-stained area in the aAb$^+$ group. This difference was due to a higher occurrence of larger areas of HA staining (>500 μm^2) and a lower occurrence of smaller HA-stained areas (500 μm^2) than in aAb$^-$ controls (p<0.001, one-way ANOVA). We used the range of HA-stained areas in the control samples to define an upper cut-off value for 'normal' HA staining, set at 3 SD above the mean of the controls, as it should include >99% of values typical of aAb$^-$ controls. Dividing the 15 aAb$^+$ donors using this threshold yielded two distinct groups (Fig. 2e, ESM Fig. 1 and ESM Fig. 2a). One group, consisting of eight aAb$^+$ donors (aAb$^+$HA^{low}) was not different from the aAb$^-$ controls (p>0.05, Mann–Whitney *U* test), while the other group, consisting of seven aAb$^+$ donors (aAb$^+$HA^{high}) had HA deposits in their islets. These seven donors were at different stages of islet autoimmunity since three of these were single aAb$^+$ and four were double aAb$^+$. In tissue from these donors, the mean islet HA-stained area was fourfold larger than in the other donors (1000 ± 240 μm^2 vs 250 ± 20 μm^2; Fig. 2e). The aAb$^+$HA^{high} tissues also showed a greater prevalence of islets highly rich in HA (21% of these islets contained the largest HA-stained areas [of >2000 μm^2] vs <1% in the controls (Fig. 2f). Moreover, in these tissues, islet HA$^+$ areas measuring 6000 to 28,000 μm^2 were frequently observed, while such areas were not present in the aAb$^-$ controls and aAb$^+$HA^{low} tissues (ESM Fig. 1).

We found a positive association between the amount of islet HA staining and the number of aAbs, but there was no association between the amount of islet HA staining and donor age

(Fig. 2e, f and ESM Fig. 2b). The islet HA-stained areas in tissues from single-aAb$^+$ donors were, on average, 1.6-fold greater than in the aAb$^-$ controls. This increase in size was attributable to the HA abundance in three single-aAb$^+$ donors who exhibited 2.7- and 3.4-fold larger islet HA-stained areas vs the aAb$^-$ group or the other seven single-aAb$^+$ donors, respectively ($p<0.01$). Overall, the double-aAb$^+$ group also exhibited larger amounts of islet HA staining compared with the single-aAb$^+$ or aAb$^-$ groups. This was a result of the prominent HA deposition in four of the five donors in this group, which resulted in islet HA$^+$ areas that were four- and fivefold larger vs the single-aAb$^+$ donors or aAb$^-$ control group, respectively ($p<0.01$). The increase in islet HA area in the aAb$^+$HA^{high} tissues was not determined by islet size. Overall, the mean islet areas in aAb$^+$ donors were within the range of aAb$^-$ controls (ESM Fig. 3).

Islet HA deposits form in the absence of insulitis and are the sites of immune-cell infiltrates

Among the seven aAb$^+$HA^{high} tissues, three from single-aAb$^+$ donors and one from a double-aAb$^+$ donor did not show insulitis (Fig. 3). The scarce islet-associated LCA$^+$ cells present in these four HA-rich tissues occurred in single units. Insulitis was detected in the three remaining tissues from donors positive for two aAbs (Fig. 3c,d,g–i). In these three aAb$^+$HA^{high}LCA^{high} tissues, HA had accumulated in the majority of the islets (Fig. 4d and ESM Fig. 4a). However, LCA$^+$ cells were located in only 13%, 14% and 28% of the islets in each of these tissues (Fig. 3i). The markedly lower prevalence of islets with LCA$^+$ cells vs that of HA-rich islets indicates that HA accumulation progresses independently of immune-cell infiltration, even in tissues that eventually develop insulitis. Further assessment of islet HA quantity in relation to insulitis in the three aAb$^+$HA^{high}LCA^{high} tissues revealed that the insulitis-free islets contained less HA staining than neighbouring islets with insulitis (3.4-fold), yet more than the islets in the other four aAb$^+$HA^{high} tissues (2.4-fold; see ESM Fig. 4b). Furthermore, the islet-infiltrating immune cells were located almost exclusively in the islets with substantial amounts of islet HA deposits (Fig. 4 and ESM Fig. 4a). In the three aAb$^+$HA^{high}LCA^{high} tissues, about one third of the islets exhibited HA-stained areas larger than 2000 μm^2 and 60% of these hosted immune cells. By contrast, such areas were found in only 8% of the islets in the four aAb$^+$HA^{high} tissues without insulitis and their mean size was significantly smaller than in the aAb$^+$HA^{high}LCA^{high} tissues (3200±800 μm^2 vs 6600±4700 μm^2; $p<0.001$). In the three aAb$^+$HA^{high}LCA^{high} tissues, CD68$^+$ and CD3$^+$ cells were frequently found in islets with LCA$^+$ cells (ESM Fig. 4c). Scarce CD20$^+$ or CD11c$^+$ cells were detected (in 'Donor 1' only), and were observed in the regions of insulitis, together with other immune cells (ESM Fig. 4c). These data may indicate that cells from both myeloid and lymphoid lineage might be attracted by islet HA. The lower frequency of CD20$^+$ and CD11c$^+$ cells vs that of CD68$^+$ and CD3$^+$ cells may indicate that occurrence of the former may be determined by a specific composition of the HA-rich islet ECM and/or the presence of other immune-cell types in islets.

The formation of large HA deposits in the three tissues with insulitis was not associated with greater numbers of LCA$^+$ cells in the non-islet region compared with control tissues. Also, the relative percentage of HA$^+$ areas in the non-islet compartment in the aAb$^+$HA^{high} group overall were not significantly different from those in the control group (ESM Fig. 2c,d).

Relationship between human islet HA and beta cell mass

The formation of HA deposits in islets of aAb$^+$ donors was not associated with changes in the size of the beta cell population (Fig. 5a–c). Apoptotic cells with TUNEL$^+$ nuclei were not detected in the endocrine compartment in any of the tissues from either the aAb$^-$ or aAb$^+$ groups. Also, the rate of beta cell proliferation did not differ between these two groups ($0.1\pm0.1\%$ in both). Beta cell mass varied among both aAb$^-$ and aAb$^+$ donors and was not related to the extent of HA staining. Interestingly, there was little variation in the size of the relative pancreas insulin$^+$ areas between the two groups, indicating that much of the variability in beta cell mass was due to differences in pancreas weight rather than islet density (Fig. 5d).

Islet HA deposits form in the presence of aAbs but are not HLA-related

Previous work indicated that the presence of islet aAbs is HLA-associated, while the progression from aAb positivity to clinical disease is not [28, 29]. Therefore, we next examined the extent of islet HA deposition in relation to HLA. Islets from two of nine donors with the HLA haplotype *DR4-DQ8* (*DRB1*04-DQA1*0301-DQB1*0302*), which is strongly associated with type 1 diabetes [30, 31], had substantial amounts of HA staining. Tissues from three of 12 donors with HLA haplotypes often considered protective for type 1 diabetes (*DRB1*0401-DQA1*0301-DQB1*0301*, *DRB1*1501-DQA1*0102-DQB1*0603* and *DRB1*0401-DQA1*0301-DQB1*0301*) and from two of seven donors with HLA haplotypes conferring neutral risk (*DRB1*0101-DQA1*0101-DQB1*0501* and *DRB1*0701-DQA1*0201-DQA2*0201*) also exhibited larger HA$^+$ areas vs controls (ESM Fig. 5 and ESM Table 1). Thus, overall, the presence of the HA-stained deposits was not associated with HLA haplotype.

In summary, as illustrated in Fig. 6, a subset of single- and double-aAb$^+$ donors (donors 1–7) showed prominent islet HA deposits. The HA-rich tissues containing the largest quantities of islet HA (donors 1– 3) exhibited insulitis. Tissues from the other aAb$^+$ donors (donors 8–15), who were mostly single aAb$^+$, did not exhibit insulitis and did not differ from the aAb$^-$ control donors with respect to the quantities and distribution of islet HA, or beta cell mass (ESM Fig. 6).

Islet HA deposition precedes insulitis in presymptomatic DR*Lyp/Lyp* rats

The DR*Lyp/Lyp* rat islets were insulitic-cell free during the first 8 weeks of age (insulitis grade 0; ESM Table 3). The insulitic infiltrates appeared at 9–10 weeks of age (grade 1, inaugural insulitis). Subsequently, these infiltrates gradually expanded around and within islets (grade 2, invasive insulitis), and then spread throughout them (grade 3, destructive insulitis). In this last stage, the islets showed massive beta cell loss (ESM Fig. 7a,b), which typically leads to hyperglycaemia within 24–48 h [22, 23]. We first examined whether HA accumulates in islets prior to the appearance of insulitic cells, and then assessed the initiation and progression of insulitis, and beta cell mass, as a function of the amount of islet HA in DR*Lyp/Lyp* rats during the progression to hyperglycaemia.

At 6 weeks of age, the quantities of islet HA staining in the DR*Lyp/Lyp* rats did not differ from those in the DR*Lyp*/+ (ESM Fig. 7c) or DR+/+ controls (data not shown). In addition,

the distribution of islet HA staining did not differ between the groups (data not shown). Islet HA deposits had developed both around and within islets in 7–8-week-old DR*Lyp/Lyp* rats, which exhibited threefold and 2.4-fold larger islet HA$^+$ areas compared with 6-week-old DR*Lyp/Lyp* and control rats, respectively (7–8-week-old DR*Lyp/Lyp*, 2370±170 μm^2; 6-week-old DR*Lyp/Lyp*, 800±50 μm^2; control, 1010±40 μm^2; Fig. 7, ESM Fig. 7c and ESM Fig. 8a,b). However, these 7–8-week-old DR*Lyp/Lyp* rats did not show any islet-associated LCA$^+$ cells (Fig. 7). Thus, in presymptomatic DR*Lyp/Lyp* rats, islet HA deposits form before the appearance of insulitic cells.

In the 9–10-week-old DR*Lyp/Lyp* rats, islet HA-stained areas were, on average, twice as large as those of their 7–8-week-old DR*Lyp/Lyp* littermates (4980 ± 500 μm^2 vs 2370 ± 170 μm^2; Fig. 7k), while the SYN$^+$ islet areas were smaller (ESM Fig. 8f). This increase in HA area size was due to a higher prevalence of islets rich in HA and the formation of large HA deposits measuring 8000–16,000 μm^2, which were not present in younger rats (data not shown). At this age, the first insulitic cells appeared and were embedded within the largest HA accumulations. This suggests that HA-rich areas are the sites of immune-cell entry into islets. The islet HA$^+$ areas were larger in DR*Lyp/Lyp* rats at 10–11 weeks of age vs at 9–10-weeks of age (1.5-fold: 7220 ± 880 μm^2 vs 4980 ± 500 μm^2; Fig. 7) and measured up to 30,000 μm^2, indicating a massive deposition of islet HA. This was associated with exacerbation of insulitis, since most islets exhibited a higher degree of immune-cell infiltration.

The initial accumulation of HA in 7–8-week-old DR*Lyp/Lyp* rat islets was not associated with a significant loss of beta cells (Fig. 7 and ESM Fig. 8b,c; $p>0.05$, Spearman's rank correlation test). In rats exhibiting abundant islet HA staining and grade 1 insulitis, the beta cell mass was reduced to 55% of that in the controls. With further expansion of the HA deposits and progression to invasive insulitis, the size of the beta cell population continued to decrease. HA remained abundant in rats with destructive insulitis, which had lost 60% of their islet mass as compared with DR*Lyp/Lyp* rats with grade 0 insulitis (1 ± 0.3 mg vs 2.5 ± 1 mg; $p<0.01$) and 85% of beta cells (ESM Fig. 8c–e).

Discussion

HA is a major component of the ECM that amasses in chronic inflammatory lesions, where HA exerts proinflammatory effects as a key regulator of leucocyte recruitment to the site of injury [19, 20, 32–34]. Our previous observation of abundant HA in human islets and regions of insulitis in type 1 diabetes implicated HA in the pathogenesis of disease [17]. Here, we investigated whether the accumulation of HA in islets is an early and critical step in the pathogenetic process of insulitis.

We report that HA deposits form in islets in a subset of aAb$^+$ donors in the absence of insulitis. We also show that, on average, double-aAb$^+$ donors exhibited larger islet HA deposits than those positive for a single aAb. These observations reveal that islet immune-cell infiltrates are not required for initial islet HA deposition, and that islet HA deposits expand along with increasing number of islet aAbs, which indicates progression of autoimmunity. It is important to point out that both the largest islet HA deposits and insulitis

were observed in the double-aAb$^+$ donors who carried the highly susceptible HLA genotype and were under 40 years of age. Essentially, all individuals with multiple islet aAbs subsequently progress to clinically overt diabetes [35]. Although progression to clinical onset of diabetes occurs at different rates, we suggest that the seven aAb$^+$ donors exhibiting prominent HA deposits were in a stage of rapid progression of the pathogenic process.

In presymptomatic DR*Lyp/Lyp* rats, initial islet HA deposition predates the appearance of insulitic cells. This finding, together with our observation of islet HA deposits in the absence of islet immune-cell infiltrates in aAb$^+$ donors, indicates that the process of HA accumulation in islets can occur independently of, and prior to, insulitis. To what extent this accumulation would have eventually contributed to the development of insulitis in the subset of single-aAb$^+$ donors with islet HA deposits, had they lived longer, is not possible to determine. Nonetheless, these results suggest that the formation of islet HA deposits may be a prerequisite for the initial adhesion of insulitic cells and subsequent infiltration of islets and, thus, could potentially be considered causal. Support for an HA–insulitis causal relationship comes from in vitro studies that indicated that an HA-rich ECM, generated by activated human fibroblasts, endothelial or smooth muscle cells, controls the migration of human mononuclear leukocytes [34, 36, 37]. Also, our observations in BB rats are in line with the finding that HA accumulation precedes the inflammatory infiltrate in the intestinal mucosa in mice with induced experimental colitis [38].

We point out a relationship between the extensiveness of islet HA accumulation and the degree of insulitis since, in BB rats, the amount of islet HA staining positively correlates with the continuum of insulitis, from inaugural to invasive. Immune cells were first observed in the islets of 7–8-week old DR*Lyp/Lyp* rats in which islet HA-stained areas had increased 2.4-fold, on average, vs younger rats. Also, in both humans and BB rats, the immune-cell infiltrates were situated within the largest HA accumulations in islets. These findings indicate that the precursory islet HA build-up may determine the sites of subsequent immune-cell entry into islets and that insulitis initiates in islets that have accumulated a 'critical' mass of HA. Additional islet HA deposition was concurrent with expansion of insulitic infiltrates inside islets, which suggests that the continuous amassment of HA may also influence the advancement of insulitis.

While the initial HA accumulation was not associated with a significant reduction in beta cell mass, the DR*Lyp/Lyp* rats with HA-abundant deposits and grade 1 insulitis exhibited a considerable loss of beta cells. The consequences of HA deposition on beta cell survival remain to be determined. In the presence of insulitis, it is difficult to dissect the impact of the accumulated HA from that of the immune cells [12, 39–41]. However, it can be speculated that changes in islet ECM properties, conferred by continual HA deposition, might affect beta cell viability via HA-induced signalling pathways and cellular responses in islets. Also, in synergy with the insulitic cells and secreted cytokines, abundant HA may create an inflammatory microenvironment that is detrimental to beta cells.

Human islets with abundant HA were not localised in specific parts of the human pancreas and their uneven distribution is reminiscent of the 'patchy' pattern of insulitis described in type 1 diabetes [1, 9, 11]. We previously found a similar distribution pattern of HA-rich

islets and insulitis in tissues from donors with type 1 diabetes [17]. These observations were reproduced in prediabetic and diabetic BB rats in the present study, in which the location of the largest islet HA deposits served as a blueprint for islet immune-cell infiltration. The complete overlap in the localisation of islets highly enriched in HA and insulitis reinforces their close relationship, which, from initially being potentially causative, might have progressed into an interdependent partnership.

In conclusion, this study indicates that islet HA accumulation is an early event in the pathogenesis of autoimmune diabetes. Our novel observations, remarkably consistent in both humans with ongoing islet autoimmunity and diabetes-prone BB rats in the preclinical stage of the disease, support our proposal of a crucial role of islet HA in the inception and promotion of islet inflammation in type 1 diabetes [16]. Therefore, additional studies are warranted to explore the underlying mechanisms that regulate HA mass in islets and the interactions between HA and islet cells or immune cells. Clarifying these molecular mechanisms will be important in developing therapeutic interventions that target HA accumulation with the aim to stop the development of insulitis.

Supplementary Material

Refer to Web version on PubMed Central for supplementary material.

Acknowledgments

Abbreviations

aAb	Autoantibody
BB	BioBreeding
ECM	Extracellular matrix
HA	Hyaluronan
LCA	Leucocyte common antigen
SYN	Synaptophysin

References

[1]. Atkinson MA, Eisenbarth GS, Michels AW (2014) Type 1 diabetes. Lancet 383(9911): 69–82. 10.1016/S0140-6736(13)60591-7 [PubMed: 23890997]

[2]. Eisenbarth GS (1986) Type I diabetes mellitus. A chronic autoimmune disease. N Engl J Med 314(21): 1360–1368. 10.1056/NEJM198605223142106 [PubMed: 3517648]

[3]. Insel RA, Dunne JL, Atkinson MA, et al. (2015) Staging presymptomatic type 1 diabetes: a scientific statement of JDRF, the Endocrine Society, and the American Diabetes Association. Diabetes Care 38(10): 1964–1974. 10.2337/dc15-1419 [PubMed: 26404926]

[4]. Couper JJ, Haller MJ, Greenbaum CJ, et al. (2018) ISPAD Clinical Practice Consensus Guidelines 2018: stages of type 1 diabetes in children and adolescents. Pediatr Diabetes 19 (Suppl 27): 20–27. 10.1111/pedi.12734 [PubMed: 30051639]

[5]. Bingley PJ, Bonifacio E, Williams AJ, Genovese S, Bottazzo GF, Gale EA (1997) Prediction of IDDM in the general population: strategies based on combinations of autoantibody markers. Diabetes 46(11): 1701–1710 [PubMed: 9356015]

[6]. Gorus FK, Keymeulen B, Veld PA, Pipeleers DG (2013) Predictors of progression to type 1 diabetes: preparing for immune interventions in the preclinical disease phase. Expert Rev Clin Immunol 9(12): 1173–1183. 10.1586/1744666X.2013.856757 [PubMed: 24215407]

[7]. Ziegler AG, Rewers M, Simell O, et al. (2013) Seroconversion to multiple islet autoantibodies and risk of progression to diabetes in children. JAMA 309(23): 2473–2479. 10.1001/jama.2013.6285 [PubMed: 23780460]

[8]. Wherrett DK, Chiang JL, Delamater AM, et al. (2015) Defining pathways for development of disease-modifying therapies in children with type 1 diabetes: a consensus report. Diabetes Care 38(10): 1975–1985. 10.2337/dc15-1429 [PubMed: 26404927]

[9]. Gepts W (1965) Pathologic anatomy of the pancreas in juvenile diabetes mellitus. Diabetes 14(10): 619–633 [PubMed: 5318831]

[10]. Pipeleers D, Ling Z (1992) Pancreatic beta cells in insulin-dependent diabetes. Diabetes Metab Rev 8(3): 209–227 [PubMed: 1292912]

[11]. In't Veld P (2011) Insulitis in human type 1 diabetes: the quest for an elusive lesion. Islets 3(4): 131–138 [PubMed: 21606672]

[12]. Roep BO (2003) The role of T cells in the pathogenesis of type 1 diabetes: from cause to cure. Diabetologia 46(3): 305–321. 10.1007/s00125-003-1089-5 [PubMed: 12687328]

[13]. Coppieters KT, Dotta F, Amirian N, et al. (2012) Demonstration of islet-autoreactive CD8 T cells in insulitic lesions from recent onset and long-term type 1 diabetes patients. J Exp Med 209(1): 51–60. 10.1084/jem.20111187 [PubMed: 22213807]

[14]. Campbell-Thompson M, Fu A, Kaddis JS, et al. (2016) Insulitis and β-cell mass in the natural history of type 1 diabetes. Diabetes 65(3): 719–731. 10.2337/db15-0779 [PubMed: 26581594]

[15]. Morgan NG, Richardson SJ (2018) Fifty years of pancreatic islet pathology in human type 1 diabetes: insights gained and progress made. Diabetologia. 10.1007/s00125-018-4731-y

[16]. Bogdani M (2016) Thinking outside the cell: a key role for hyaluronan in the pathogenesis of human type 1 diabetes. Diabetes 65(8): 2105–2114. 10.2337/db15-1750 [PubMed: 27456615]

[17]. Bogdani M, Johnson PY, Potter-Perigo S, et al. (2014) Hyaluronan and hyaluronan-binding proteins accumulate in both human type 1 diabetic islets and lymphoid tissues and associate with inflammatory cells in insulitis. Diabetes 63(8): 2727–2743. 10.2337/db13-1658 [PubMed: 24677718]

[18]. Laurent TC, Laurent UB, Fraser JR (1996) The structure and function of hyaluronan: an overview. Immunol Cell Biol 74(2): A1–A7. 10.1038/icb.1996.32 [PubMed: 8724014]

[19]. Petrey AC, de la Motte CA (2014) Hyaluronan, a crucial regulator of inflammation. Front Immunol 5: 101 10.3389/fimmu.2014.00101 [PubMed: 24653726]

[20]. Wang A, de la Motte C, Lauer M, Hascall V (2011) Hyaluronan matrices in pathobiological processes. FEBS J 278(9): 1412–1418. 10.1111/j.1742-4658.2011.08069.x [PubMed: 21362136]

[21]. Mordes JP, Bortell R, Blankenhorn EP, Rossini AA, Greiner DL (2004) Rat models of type 1 diabetes: genetics, environment, and autoimmunity. ILAR J 45(3): 278–291 [PubMed: 15229375]

[22]. Fuller JM, Bogdani M, Tupling TD, et al. (2009) Genetic dissection reveals diabetes loci proximal to the gimap5 lymphopenia gene. Physiological genomics 38(1): 89–97. 10.1152/physiolgenomics.00015.2009 [PubMed: 19351909]

[23]. Bogdani M, Henschel AM, Kansra S, et al. (2013) Biobreeding rat islets exhibit reduced antioxidative defense and N-acetyl cysteine treatment delays type 1 diabetes. J Endocrinol 216(2): 111–123. 10.1530/joe-12-0385 [PubMed: 23111281]

[24]. Toole BP, Yu Q, Underhill CB (2001) Hyaluronan and hyaluronan-binding proteins. Probes for specific detection. Methods Mol Biol 171: 479–485. 10.1385/1-59259-209-0:479 [PubMed: 11450261]

[25]. Hellman B, Angervall L (1961) The frequency distribution of the number and volume of the islets of Langerhans in man: studies in diabetes of early onset, insuloma and acromegaly. Acta Pathol Microbiol Scand 53: 230–236. 10.1111/j.1699-0463.1961.tb00405.x [PubMed: 13906265]

[26]. Kim A, Miller K, Jo J, Kilimnik G, Wojcik P, Hara M (2009) Islet architecture: a comparative study. Islets 1(2): 129–136. 10.4161/isl.1.2.9480 [PubMed: 20606719]

[27]. Campbell-Thompson ML, Atkinson MA, Butler AE, et al. (2013) The diagnosis of insulitis in human type 1 diabetes. Diabetologia 56(11): 2541–2543. 10.1007/s00125-013-3043-5 [PubMed: 24006089]

[28]. Ziegler AG, Nepom GT (2010) Prediction and pathogenesis in type 1 diabetes. Immunity 32(4): 468–478. 10.1016/j.immuni.2010.03.018 [PubMed: 20412757]

[29]. Redondo MJ, Geyer S, Steck AK, et al. (2018) A type 1 diabetes genetic risk score predicts progression of islet autoimmunity and development of type 1 diabetes in individuals at risk. Diabetes Care 41(9): 1887–1894. 10.2337/dc18-0087 [PubMed: 30002199]

[30]. Concannon P, Rich SS, Nepom GT (2009) Genetics of type 1A diabetes. N Engl J Med 360(16): 1646–1654. 10.1056/NEJMra0808284 [PubMed: 19369670]

[31]. Noble JA, Erlich HA (2012) Genetics of type 1 diabetes. Cold Spring Harb Perspect Med 2(1): a007732 10.1101/cshperspect.a007732 [PubMed: 22315720]

[32]. Jiang D, Liang J, Noble PW (2011) Hyaluronan as an immune regulator in human diseases. Physiol Rev 91(1): 221–264. 10.1152/physrev.00052.2009 [PubMed: 21248167]

[33]. Mummert ME (2005) Immunologic roles of hyaluronan. Immunol Res 31(3): 189–206. 10.1385/IR:31:3:189 [PubMed: 15888911]

[34]. Evanko SP, Potter-Perigo S, Bollyky PL, Nepom GT, Wight TN (2012) Hyaluronan and versican in the control of human T-lymphocyte adhesion and migration. Matrix Biol 31(2): 90–100. 10.1016/j.matbio.2011.10.004 [PubMed: 22155153]

[35]. Bingley PJ, Boulware DC, Krischer JP, the Type 1 Diabetes TrialNet Study Group (2016) The implications of autoantibodies to a single islet antigen in relatives with normal glucose tolerance: development of other autoantibodies and progression to type 1 diabetes. Diabetologia 59(3): 542–549. 10.1007/s00125-015-3830-2 [PubMed: 26676824]

[36]. de La Motte CA, Hascall VC, Calabro A, Yen-Lieberman B, Strong SA (1999) Mononuclear leukocytes preferentially bind via CD44 to hyaluronan on human intestinal mucosal smooth muscle cells after virus infection or treatment with poly(I.C). J Biol Chem 274(43): 30747–30755 [PubMed: 10521464]

[37]. Lauer ME, Mukhopadhyay D, Fulop C, de la Motte CA, Majors AK, Hascall VC (2009) Primary murine airway smooth muscle cells exposed to poly(I,C) or tunicamycin synthesize a leukocyte-adhesive hyaluronan matrix. J Biol Chem 284(8): 5299–5312. 10.1074/jbc.M807965200 [PubMed: 19088077]

[38]. Kessler S, Rho H, West G, Fiocchi C, Drazba J, de la Motte C (2008) Hyaluronan (HA) deposition precedes and promotes leukocyte recruitment in intestinal inflammation. Clin Transl Sci 1(1): 57–61. 10.1111/j.1752-8062.2008.00025.x [PubMed: 20443819]

[39]. Delaney CA, Pavlovic D, Hoorens A, Pipeleers DG, Eizirik DL (1997) Cytokines induce deoxyribonucleic acid strand breaks and apoptosis in human pancreatic islet cells. Endocrinology 138(6): 2610–2614. 10.1210/endo.138.6.5204 [PubMed: 9165055]

[40]. Eizirik DL, Mandrup-Poulsen T (2001) A choice of death--the signal-transduction of immune-mediated beta-cell apoptosis. Diabetologia 44(12): 2115–2133. 10.1007/s001250100021 [PubMed: 11793013]

[41]. Pinkse GG, Tysma OH, Bergen CA, et al. (2005) Autoreactive CD8 T cells associated with beta cell destruction in type 1 diabetes. Proc Natl Acad Sci U S A 102(51): 18425–18430. 10.1073/pnas.0508621102 [PubMed: 16339897]

Research in context

What is already known about this subject?

- We previously reported that an extracellular matrix rich in hyaluronan (HA) is a prominent feature of insulitis in type 1 diabetes

What is the key question?

- Does the accumulation of HA take place early in type 1 diabetes and prior to insulitis?

What are the new findings?

- Large HA deposits are present in islets in a subset of autoantibody (aAb)$^+$ organ donors, and are the sites where immune cells infiltrate the islets. The abundance of these deposits is associated with the number of aAbs (single double aAb positivity) but not with HLA genotype

- Islet HA deposits form both in pancreases in which insulitis is not detected and in immune-cell-free islets in pancreases that exhibit insulitis, which indicates that islet immune-cell infiltrates are not required for initial islet HA deposition

- Incipient HA accumulation precedes islet immune-cell infiltration in presymptomatic BioBreeding DR*Lyp/Lyp* rats. Continual amassment of HA is associated with the appearance of the insulitic cells and positively correlates with the degree of insulitis

How might this impact on clinical practice in the foreseeable future?

- Our findings implicate accumulation of HA as a marker of early disease and as a mediator driving immune cell migration into islets, which opens the door for potential novel therapeutic interventions that target HA accumulation
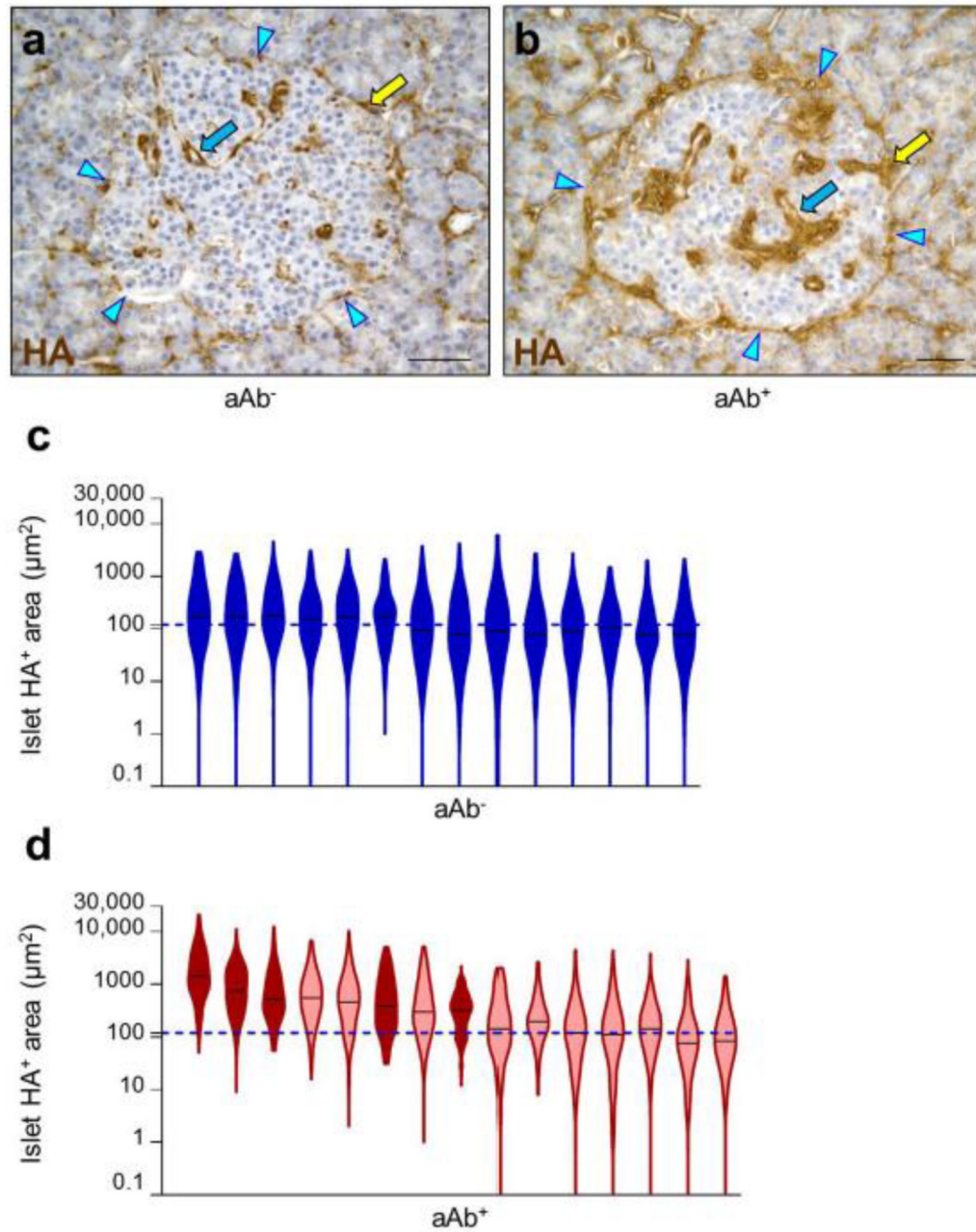
Fig. 1.
Islet HA deposits in aAb$^+$ donors. HA staining (brown) in islets from (**a**) aAb$^-$ and (**b**) aAb$^+$ donors. Yellow arrows indicate HA at the islet periphery, while blue arrows indicate HA within the islet. Arrowheads point to the islet border. Scale bars, 50 μm. (**c, d**) Violin plots of HA$^+$ areas measured in islets from each donor for aAb$^-$ donors (**c**) and aAb$^+$ donors (**d**; light red, single-aAb$^+$; dark red, double-aAb$^+$). Islet HA$^+$ areas are shown on a log$_{10}$ scale. The dotted horizontal lines indicate the median of HA$^+$ area in the control aAb$^-$ group
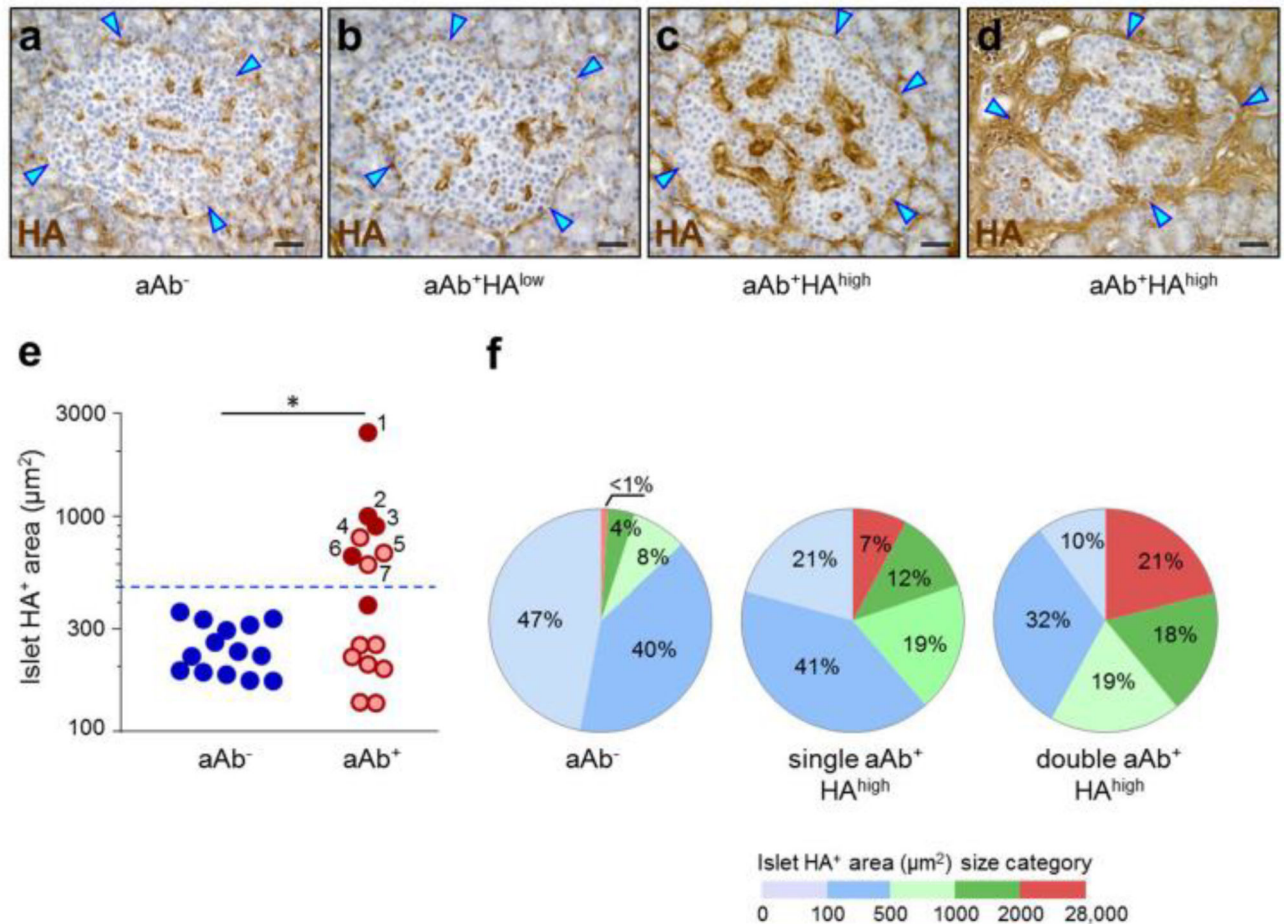
Fig. 2.
HA accumulates in islets from a subset of aAb⁺ donors. HA staining (brown) in islets from
(**a**) aAb⁻, (**b, c**) single-aAb⁺ and (**d**) double-aAb⁺ donors. Arrowheads point to the islet
border. Scale bars, 50 μm. (**e**) Morphometric quantification of islet HA⁺ areas, shown on a
$\log_{10}$ scale. Each circle denotes an individual donor; blue, aAb⁻; light red, single-aAb⁺; dark
red, double-aAb⁺. Data are mean values of islet HA⁺ areas for each individual donor. The
numbers (1–7) indicate the aAb⁺HA^{high} tissues ranked according to the size of islet HA⁺
areas. The dotted horizontal line indicates the upper cut-off value (mean of HA⁺ area in aAb
⁻control + 3 SD). In total, 4598, 3210 and 2272 islets from aAb⁻, single-aAb⁺ and double-
aAb⁺ donor tissues were analysed, respectively. (**f**) Islet HA⁺ area size distribution. The pie
charts represent the percentage of islets with HA⁺ areas falling within each of the HA⁺ area
size categories. Islets were analysed in aAb⁻ tissues (*n*=4598 islets) and in aAb⁺HA^{high}
tissues from *n*=3 single-aAb⁺ donors (*n*=982 islets) and *n*=4 double-aAb⁺ donors (*n*=1828
islets). *$p<0.001$,single-aAb⁺HA^{high} vs controls, and double-aAb⁺HA^{high} vs single-aAb
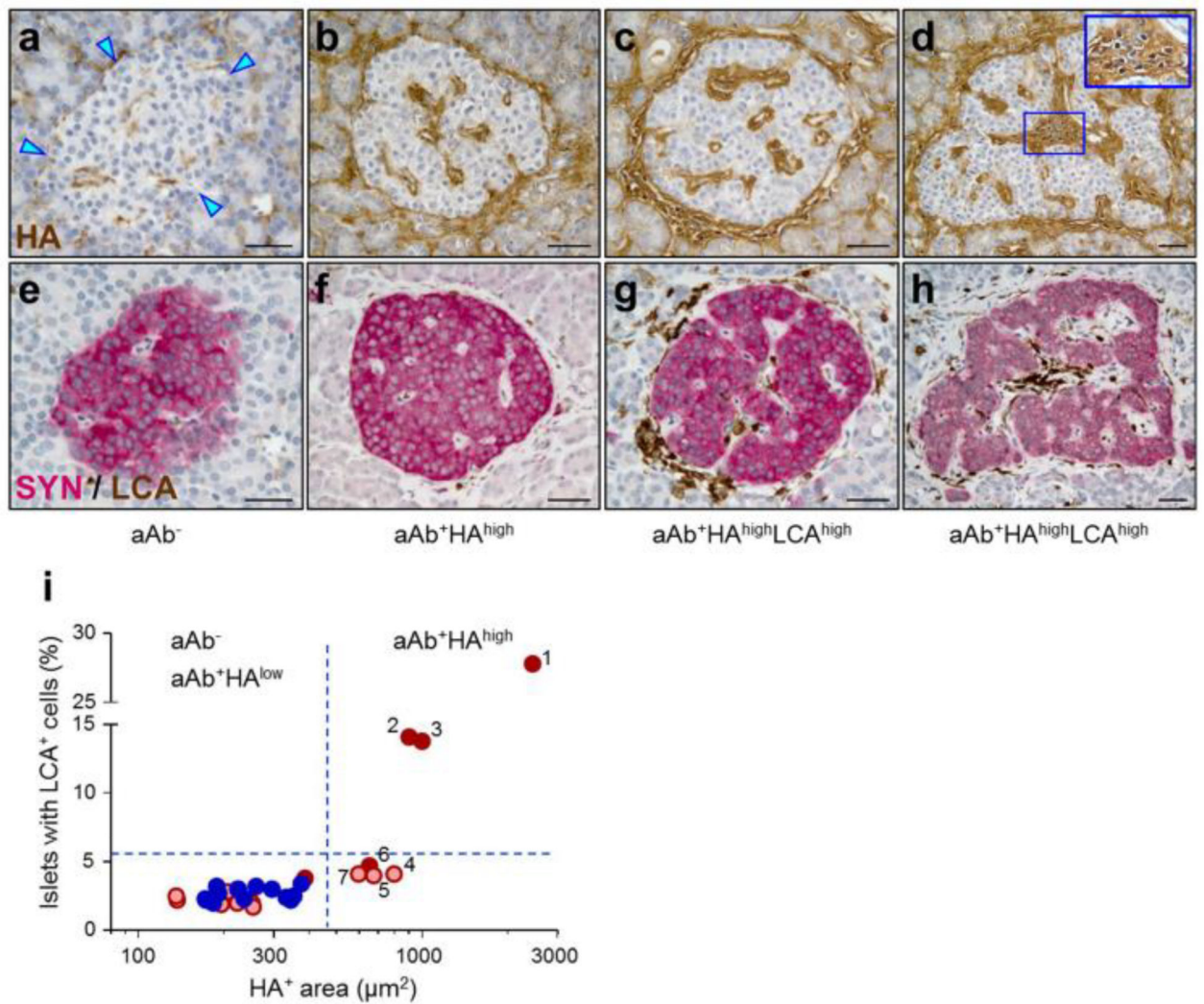⁺HA^{high} or controls; Mann–Whitney *U* test

Fig. 3.
Islet HA accumulation takes place in the absence of insulitis. HA staining (brown) in islets
from (**a**) aAb⁻ and (**b–d**) aAb⁺ donors. Arrowheads point to the islet border. The area of
insulitis in (**d**) is shown magnified in the inset. (**e–h**) Adjacent sections of the islets shown in
(**a–d**), respectively, stained for LCA (brown) and SYN (red). Scale bars, 50 μm. (**i**)
Prevalence of islets with LCA⁺ cell infiltrates plotted as a function of islet HA⁺ areas, shown
on a $\log_{10}$ scale. Each circle denotes mean values for an individual donor. The dotted lines
indicate the upper cut-off values (mean + 3 SD) of the measurements obtained from the aAb
⁻ controls. The numbers (1–7) indicate the aAb⁺HA^high tissues ranked according to the size
of islet HA⁺ areas. Blue, aAb⁻; light red, single-aAb⁺; dark red, double-aAb⁺
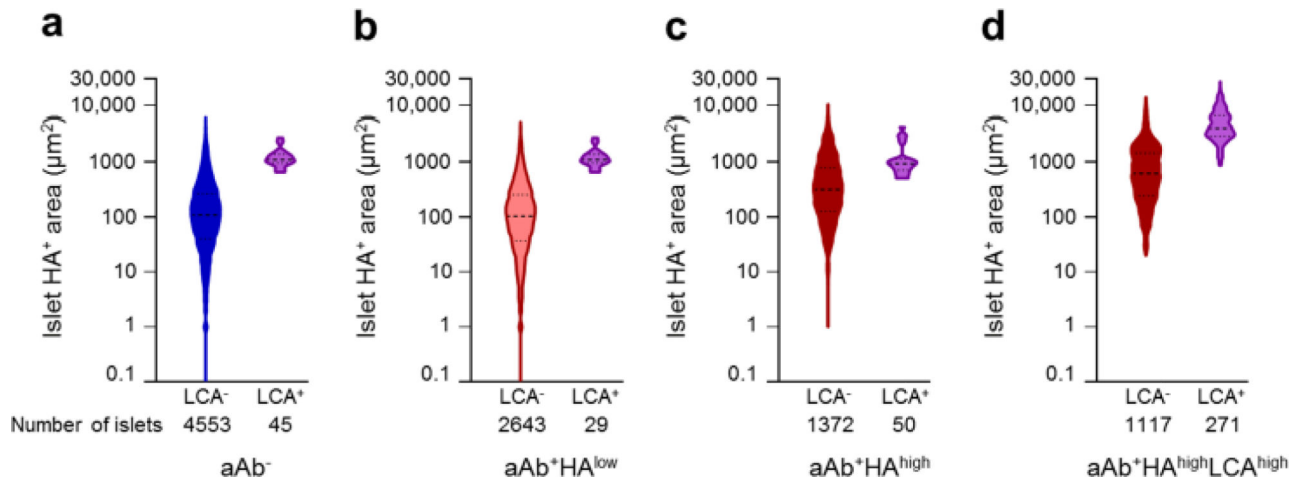
Fig.4.
Insulitis occurs exclusively in the islet regions containing the largest HA deposits. Violin plots of HA$^+$ areas in islets without (LCA$^-$) or with (LCA$^+$) immune cells for the (**a**) aAb$^-$, (**b**) aAb$^+$HA^{low}, (**c**) aAb$^+$HA^{high} and (**d**) aAb$^+$HA^{high}LCA^{high} tissues. Islet HA$^+$ areas are shown on a log$_{10}$ scale. The total number of LCA$^-$ or LCA$^+$ islets in each group is indicated. LCA$^+$ cells/100 islets: 3 ± 1 in (**a**) and (**b**); 5 ± 2 in (**c**); 47 ± 36 in (**d**)
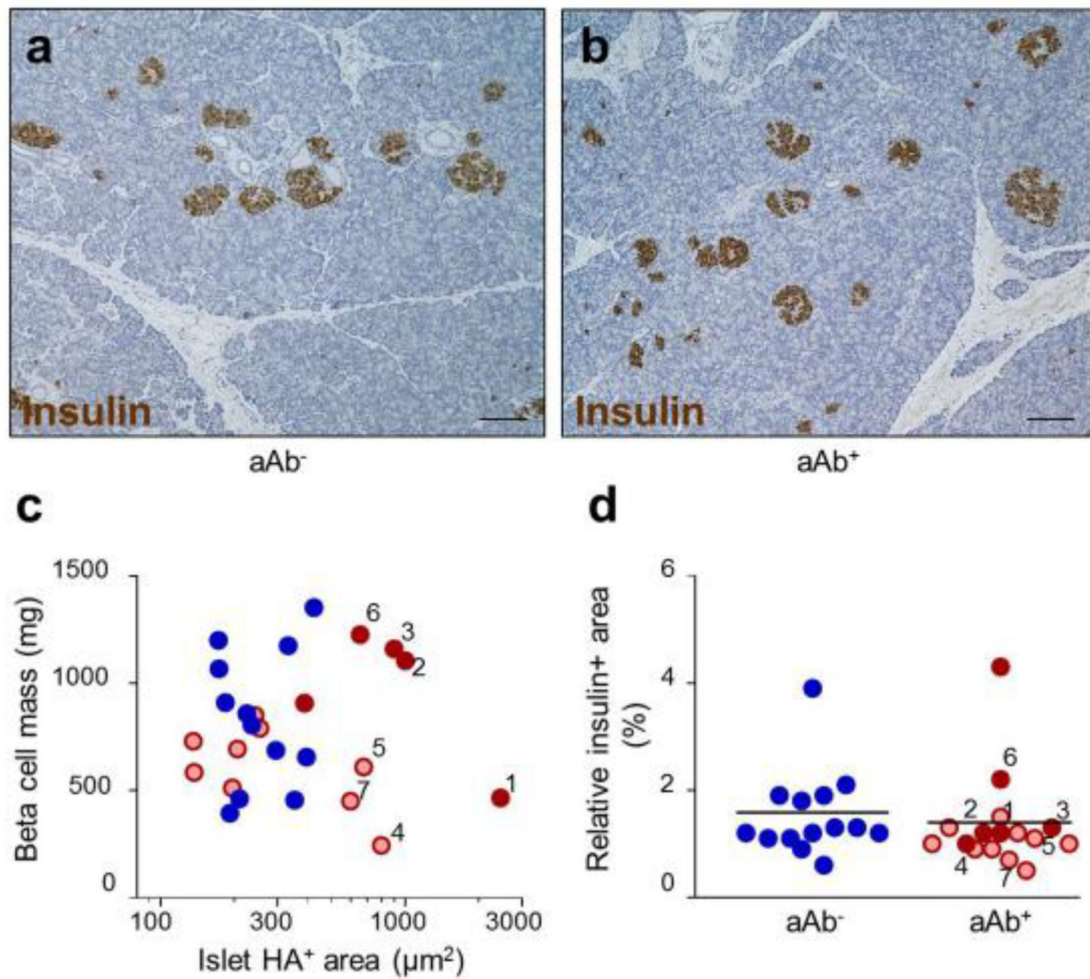
Fig. 5.
Relationship between islet HA and beta cell mass. Immunohistochemical staining for insulin (brown) in islets from (**a**) control aAb[−] and (**b**) aAb[+]HA[high] tissues. Scale bars, 100 μm. (**c**) Individual measurements of beta cell mass plotted as a function of islet HA[+] area, shown on a $\log_{10}$ scale. (**d**) Insulin[+] area relative to pancreas section area. Data are presented as the mean values of measurements for each individual donor. In (**d**), the horizontal lines represent the mean value in each group. The numbers (1–7) indicate the aAb[+]HA[high] tissues ranked according to the size of islet HA[+] areas. Blue, aAb[−]; light red, single-aAb[+]; dark red, double-aAb[+]

a

Donor	Tissue group	Islet HA+ area (μm²)	Islets with HA+ areas (%)	Islets with LCA+ cells (%)	Beta cell mass (mg)	HLA genotype	aAb
1	aAb+HAhigh	2450			470	Susceptible	GADA+ IA-2A+
2	aAb+HAhigh	1000			1100	Susceptible	IA2A+ ZnT8A+
3	aAb+HAhigh	900			1160	Protective	GADA+ mIAA+
4	aAb+HAhigh	800			610	Protective	GADA+
5	aAb+HAhigh	680			450	Neutral	GADA+
6	aAb+HAhigh	660			1230	Protective	GADA+ mIAA+
7	aAb+HAhigh	600			240	Neutral	GADA+
8	aAb+HAlow	380			910	Protective	GADA+ IA-2A+
9	aAb+HAlow	250			790	Protective	ZnT8+
10	aAb+HAlow	250			N/D	Susceptible	GADA+
11	aAb+HAlow	220			850	Susceptible	GADA+
12	aAb+HAlow	200			690	Susceptible	GADA+
13	aAb+HAlow	200			510	Neutral	GADA+
14	aAb+HAlow	140			580	Protective	GADA+
15	aAb+HAlow	140			730	Protective	GADA+

Islet HA+ area (μm²) size category

0   100   500   1000   2000   28,000
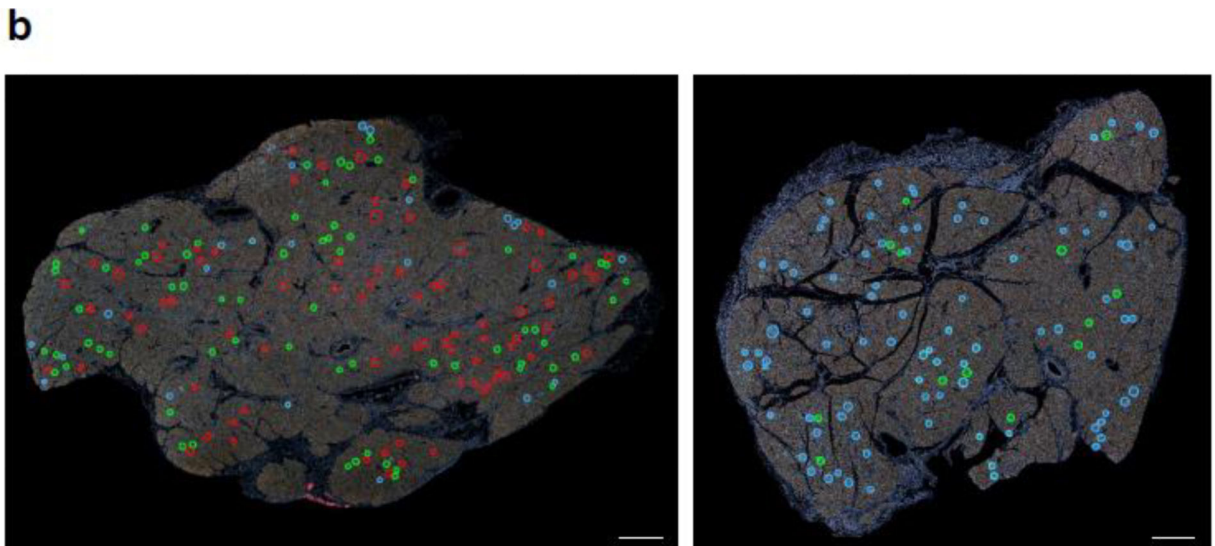
Islets with LCA+ cells (%)

b

Fig. 6.
(**a**) Islet HA$^+$ areas, insulitis and beta cell mass in individual aAb$^+$ donors. Islet HA$^+$ areas are shown as mean values obtained from the islets examined in each pancreas. Between 250 and 560 islets were analysed per pancreas. For 'islet HA$^+$ area' and 'beta cell mass', the size of each red circle is proportional to the mean value, which is indicated within the circle. The pie charts represent the percentage of islets with HA$^+$ areas falling within each of the HA$^+$ area size categories or the percentage of islets with LCA$^+$ cells. HLA genotype and aAb status are also shown for each donor. See ESM Fig. 6 for further analyses. (**b**) Whole slide images of pancreas tissue sections from donor 1 (aAb$^+$HA^{high}) and donor 13 (aAb$^+$HA^{low}). The blue, green, and red circles show the islet border and the indicate islets with HA-stained areas 500 μm^2, 501–2000 μm^2 and >2000 μm^2, respectively. Scale bars, 2000 μm. N/D, not determined
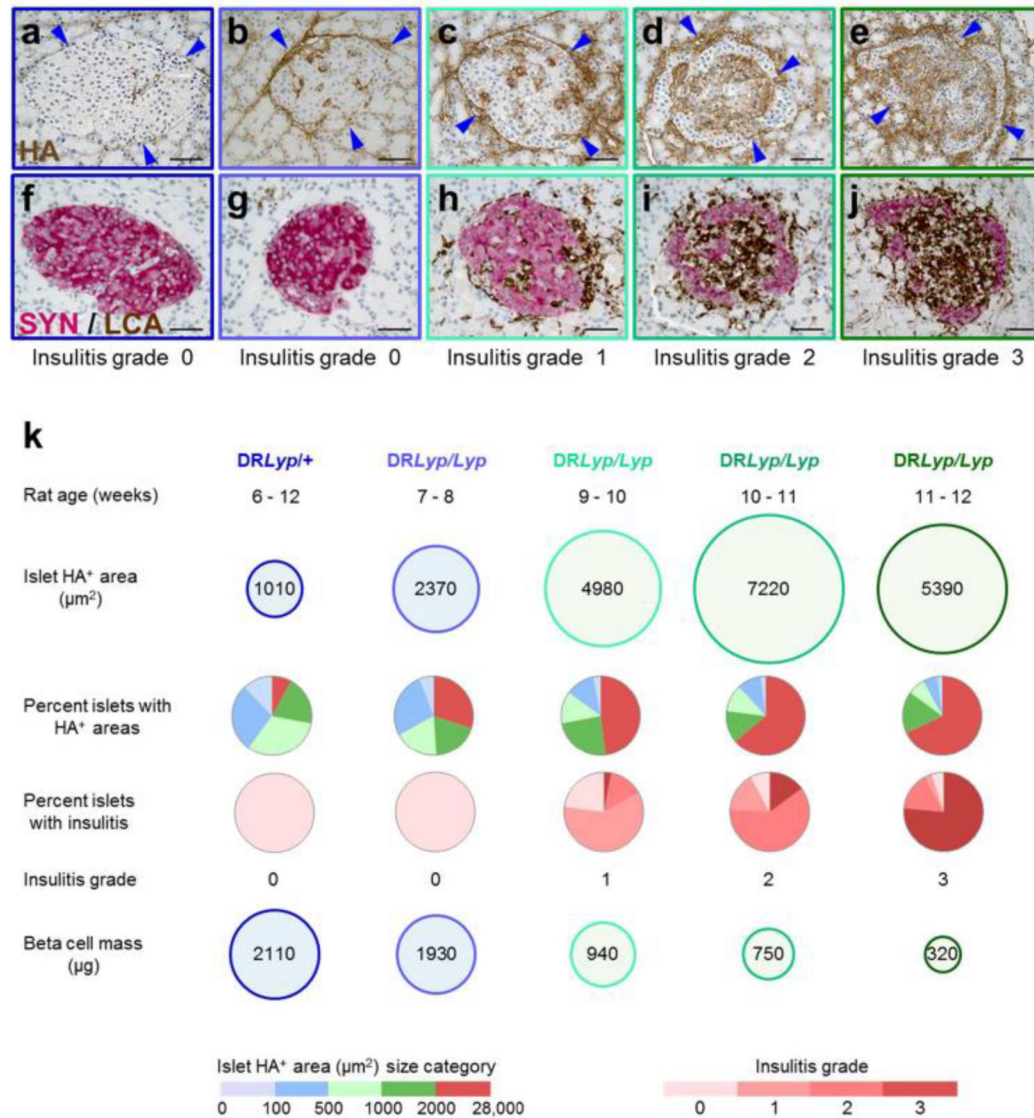
Fig. 7.
Islet HA accumulation precedes insulitis in presymptomatic DR*Lyp/Lyp* rats. (**a–e**) HA staining (brown) in islets from (**a**) diabetes-resistant DR*Lyp*/+ and (**b–e**) diabetes-prone DR*Lyp/Lyp* rats. Arrowheads point to the islet border. (**f–j**) SYN (red) staining of islets from (**f**) DR*Lyp*/+ and (**g–j**) DR*Lyp/Lyp* rats. Scale bars, 50 μm. (**k**) Islet HA⁺ areas (mean in 300–400 islets/group), islet HA⁺ area size distribution, insulitis and beta cell mass in DR*Lyp*/+ and DR*Lyp/Lyp* rats. For 'islet HA⁺ area' and 'beta cell mass', the size of each circle is proportional to the mean value, which is indicated within the circle. The pie charts in represent the percentage of islets with HA⁺ areas falling within each of the HA area size categories or the proportion of islets with insulitis grade 0, 1, 2 or 3 in the rats within each age group (see ESM Table 3 for further details)